hydrology

MDPI

Article

Understanding Dry and Wet Conditions in the Vietnamese Mekong Delta Using Multiple Drought Indices: A Case Study in Ca Mau Province

Huynh Vuong Thu Minh [1], Pankaj Kumar [2,*], Tran Van Ty [3], Dinh Van Duy [3], Tran Gia Han [4], Kim Lavane [5] and Ram Avtar [6]

1 Water Resources Department, College of Environment and Natural Resources, Can Tho University, Can Tho 900000, Vietnam
2 Institute for Global Environmental Strategies, Hayama 240-0115, Japan
3 Water Resource Engineering Faculty, College of Engineering, Can Tho University, Can Tho 900000, Vietnam
4 Environment and Natural Resources Management Department, College of Environment and Natural Resources, Can Tho University, Can Tho 900000, Vietnam
5 Environmental Engineering Department, College of Environment and Natural Resources, Can Tho University, Can Tho 900000, Vietnam
6 Faculty of Environmental Earth Science, Hokkaido University, Sapporo 060-0810, Japan
* Correspondence: kumar@iges.or.jp

Abstract: Globally, hydrometeorological hazards have large impacts to agriculture output, as well as human well-being. With climate change derived increasing frequency of extreme weather conditions, the situation has becoming more severe. This study strives to evaluate both dry and wet conditions in the Vietnamese Mekong Delta (VMD), also known as the rice basket of the Southeast Asian region. Different meteorological parameters from the last three decades were used to develop drought indices for Ca Mau province to investigate their impact on agricultural output. For this purpose, the standard precipitation index (SPI), the agricultural rainfall index (ARI), and the standardized precipitation evapotranspiration index (SPEI) were used in this study. Results highlight that Ca Mau has a peculiar characteristic of the whole VMD in that dry periods persist well into the wet season extending the duration of drought events. The role of storms, including tropical storms, and El Niño cannot be ignored as extreme events, which both change humidity, as well as rainfall. It is also found that the drought situation has caused significant damage to both rice and shrimp outputs in almost 6000 hectares. The assessment contributes to an improved understanding of the pattern of unpredictable rainfall and meteorological anomaly conditions in Ca Mau. The findings of this paper are important for both policymakers and practitioners in designing more robust plans for water resource management.

Keywords: Vietnamese Mekong Delta; droughts; Ca Mau; agriculture; SPI; ARI; SPEI

Citation: Minh, H.V.T.; Kumar, P.; Van Ty, T.; Duy, D.V.; Han, T.G.; Lavane, K.; Avtar, R. Understanding Dry and Wet Conditions in the Vietnamese Mekong Delta Using Multiple Drought Indices: A Case Study in Ca Mau Province. *Hydrology* **2022**, *9*, 213. https://doi.org/10.3390/hydrology9120213

Academic Editors: Nicholas Dercas and Mohammad Valipour

Received: 29 September 2022
Accepted: 23 November 2022
Published: 28 November 2022

1. Introduction

Drought ranks first among all natural hazards in terms of severity, duration, spatial extent, long-term socioeconomic effects, and life-related effects [1–4] since it was officially defined as an abnormal dryness caused by a precipitation deficit [2,4,5]. Drought types have been divided into four categories, namely: meteorological, agricultural, hydrological, and socioeconomic [6–9]. A meteorological, hydrological, or agricultural drought is concerned with how to measure drought as a physical phenomenon, but a socioeconomic drought is focused on supply and demand as well as the repercussions of water scarcity as they spread through socioeconomic systems [8,9].

Extreme weather events, including both dry or wet periods, present major impacts to crop production at differing levels of influence depending on the growth stage of the crop [10,11]. Hence, the combined assessment of the drought hazard and the associated

impacts on crop production, based on a probabilistic approach, is most suitable to capture the multivariate character of drought risk in agriculture [12]. Droughts usually require a minimum of two to three months to become established, but then can continue for months or years. Wilhite, a famous agronomist, also noted that the magnitude of drought impacts is closely related to precipitation distribution characteristics [13].

Many drought indices that have been developed to characterize agricultural drought are available to assist in the quantitative assessment of drought severity, heavily relying on ground-based climate data [13–16]. Agricultural drought is a natural hazard arising from insufficient crop water supply, and agricultural drought is defined as climatic variability causes a precipitation deficit, resulting in meteorological drought; the latter, when combined with high temperatures and low relative humidity, causes increased evapotranspiration, resulting in agricultural drought, i.e., a soil moisture deficit causing reduced crop yield [3,17]. However, records highlight the increasing frequency and magnitude of droughts in recent decades and mounting losses from extended droughts in agriculture [2]. Moreover, SPEI was found to be a better indicator to reflect the temporal variability of river discharge and reservoir storage. Vicente-Serrano et al. [18] compared PDSI, SPI, and SPEI for agricultural, hydrological, and ecological drought monitoring, respectively, at a global scale. Their results demonstrated that SPEI was the best drought index for capturing the impacts of drought on agricultural, hydrological, and ecological variables.

Due to the fact that agricultural output depends on soil moisture levels and access to water supplies, agriculture is often the first sector to be affected by drought [19]. When available stored water can only sustain actual evapotranspiration at a rate that is only a small percentage of the rate at which it could support actual evapotranspiration, this is when a drought in the agricultural sense begins [20].

Milanovic et al. [21] analyzed the effects of meteorological and agricultural drought across the standard precipitation index (SPI) and the agricultural rainfall index (ARI) in Serbia from 1980 to 2010. In most of the observed stations, the year 2000 had the highest drought intensity for both types of drought. Another study was conducted to assess the effects of rainfall variability on cassava growth using the agricultural rainfall index (ARI). The analysis results highlighted that the agricultural rainfall index (ARI) varied by location and month based on potential evapotranspiration [15,21]. Furthermore, the standardized precipitation evapotranspiration index (SPEI) was developed in 2010 and is now used in an increasing number of climatology and hydrology studies [22]. Based on the SPEI series, Santiago et al. updated and improved global datasets for the global real-time drought monitoring system [22]. A study conducted in China revealed that SPEI agrees with SPI, because SPEI change was dominated by precipitation change [23]. However, the method used to calculate reference evapotranspiration (PET) (e.g., the Penman-Monteith method or the Thornthwaite method) exerts a significant impact on the temporal characteristics of SPEI [23].

As mentioned above, several different types of droughts exist, and the factors or parameters that define them differ from one type to another. For example, meteorological drought is principally defined by a deficiency of precipitation from expected or "normal" over an extended period of time, while agricultural drought is best characterized by deficiencies in soil moisture, a critical factor in defining crop production potential [13]. Agricultural drought depends on the crop evapotranspiration demand and the soil moisture availability to meet this demand. Agricultural impacts of droughts are the result of short-term precipitation shortages, temperature anomalies that increase evapotranspiration demand, and soil water deficits that may adversely affect crop production. Hence, an agricultural drought index should ideally integrate the various parameters such as rainfall, temperature, evapotranspiration (ET), runoff, and other water supply indicators into a single number and provide a comprehensive picture for decision making. Agricultural drought indices should be based on soil moisture and evapotranspiration deficits and should help effectively monitor agricultural drought. The Mekong Delta in Vietnam, is also known as the rice basket of Southeast Asia. As such, hydrometeorological hazards have

huge impacts on agriculture output as well as ramifications for regional human well-being and socioeconomic development.

Ca Mau is a coastal province in the VMD that, unlike other provinces, cannot supplement fresh water from the upstream Mekong River; consequently, people's lives and production processes rely entirely on groundwater and rainfall. With climatic anomalies and extreme weather conditions increasing, compounded by the excessive extraction of groundwater, the province has been severely impacted by both drought and saltwater intrusion. Weather and natural disasters in Ca Mau province have become increasingly complicated and unpredictable in recent years, posing a threat and challenge to both agriculture and livelihood. Hence, understanding the drought phenomenon, as well as the wetness phenomenon and estimating the possibility of drought is critical for the sustainable management of agriculture and water resources in the province. Against this backdrop, this study strives to evaluate the drought events using SPI, ARI, and SPEI indices for the past three decades and assesses their impacts on the provincial agricultural sector.

2. Methods

2.1. Study Area and Data Collection

The coastal province of Ca Mau is located in the Ca Mau Peninsula, which is the southernmost part of Vietnam (Figure 1). Ca Mau of young land, that was only discovered and populated within the last 300 years. The north borders Bac Lieu and Kien Giang provinces; the east borders the East Sea with a 107 km coastline; and the west and south borders the Gulf of Thailand with a 147 km coastline. Ca Mau province's mainland territory is located at coordinates 8°34′–9°33′ N and 105°25′–104°43′ East.

Ca Mau province experiences year-round humidity due to its tropical sub-equatorial monsoon climate, with the exception of two to three reasonably dry months in the winter. Ca Mau's climate is divided into two seasons: wet season and dry season. The wet season starts from May to November, and the dry season begins from December to April the following year. Ca Mau has 165 rainy days per year, with an average annual rainfall of 2360 mm. In the wet season, the average rainfall varies little between months, ranging from 200 mm to 400 mm per month. The average temperature difference between the hottest and coldest months is about 3 °C. The average annual evaporation is around 1000 mm, with the dry season (March–April) evaporating nearly 130 mm per month. The average annual humidity is 83%, with low humidity during the dry season, especially in the month of March, when the humidity usually reduces to around 50% [24].

The Ca Mau meteorological station was used to collect monthly data on rainfall, as well as maximum, minimum, and average temperatures (T_{max}, $T_{min,}$ and T_{ave}). Indices including SPI, ARI, and SPEI were used for the meteorological drought monitoring and assessment in the study area. Between 2000 and 2019, the mean values of T_{max}, T_{min}, $T_{ave.}$, and rainfall were 31.8 °C, 25.2 °C, 27.6 °C, and 2292 mm year^{-1}, respectively. Rainfall varied the most, followed by T_{min}, T_{max}, and $T_{ave.}$, and the coefficient of variations were 0.11, 0.038, 0.036, and 0.032, respectively.

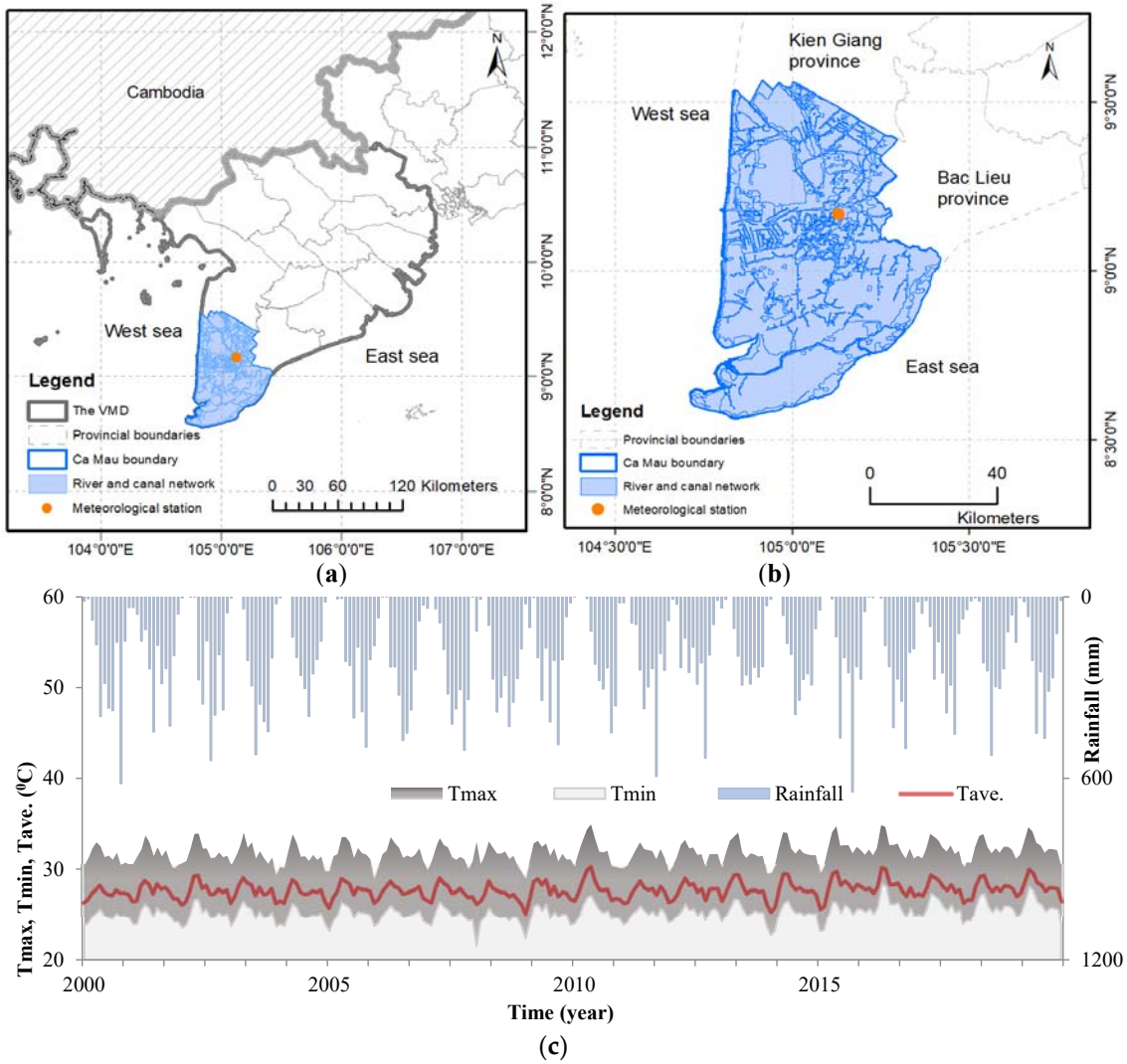

Figure 1. Location of Ca Mau province (**a**) and meteorological station (**b**); and T_{max}, T_{min}, T_{ave}, and rainfall distribution between the years 2000 and 2019 (**c**).

2.2. Data Collection and trend analysis

Monthly rainfall was collected from 1980 to 2019, and monthly average values of T_{max}, T_{min}, and $T_{ave.}$, were collected from 2000 to 2019. The Mann–Kendall test was used to evaluate the trend of data collection, SPI, ARI, and SPEI (see references [25–27]). The monthly data of T_{min}, T_{max}, and $T_{ave.}$ all slightly increased, while the monthly rainfall was seen to slightly decrease between 2000 and 2019, but not statistically significantly (Figure 1).

2.3. SPI, ARI, and SPEI Calculation

The standardized precipitation index (SPI), developed by McKee et al. (1993 and 1995) [28,29], is widely used around the world [30–34]. It was used in this study to calculate the impact of drought on agriculture and establish its frequency using time steps of 3, 6, and 9 months. For each period, the SPI estimate and the hierarchy of humidity and drought based on the SPI index were computed and graded in accordance with Formula (1) and Table 1, respectively.

$$SPI_i = \frac{(R_i - \overline{R_i})}{\sigma_i} \quad (1)$$

where R_i is rainfall in period i (3-month, 6-month, and 9-month), $\overline{R_i}$ mean annual rainfall in period i, σ_i is standard deviation on period i.

Table 1. The classification of drought and wetness according to the SPI and SPEI indices.

Drought Levels	SPI/SPEI Values	Drought Levels	SPI/SPEI Values
Normal	0–0.24	Normal	(−0.24)–0
Very slightly wet condition	0.25–0.49	Very slight drought	(−0.49)–(−0.25)
Slightly wet condition	0.5–0.99	Slight drought	(−0.99)–(−0.5)
Moderately wet condition	1–1.44	Moderate drought	(−1.44)–(−1)
Severely wet condition	1.5–1.99	Severe drought	(−1.99)–(−1.5)
Extremely wet condition	>2	Extreme drought	<(−2)

The drought begins when the SPI first falls below a negative value of 0.25 or less and ends when the SPI returns to a positive value of 0.25 or higher.

The agricultural rainfall index (*ARI*) was also used to investigate the severity and persistence of the drought in the studied area. It has been used in many previous studies [35–37]. ARI is a reliable monthly water balance indicator that is used to quantify agricultural droughts [37–39]. The ARI is calculated as follows:

$$ARI = \left(\frac{P}{ET_0}\right) \cdot 100 \quad (2)$$

where P is the monthly precipitation (mm), and ET_0 is the reference evapotranspiration (mm month^{-1}). The occurrence of drought in a given month is indicated by *ARI* values of 40. When the *ARI* varies from 40 to 200, the environment is favorable for vegetation growth and agricultural production. A month with an *ARI* greater than 200 indicates a wet month [37,38,40].

ET_0 was calculated using the original equation version of Hargreaves [41].

$$ET_0 = 0.408 \cdot 0.0023 \cdot (T_{mean} + 17.8)(T_{max} - T_{min})^{0.5}. R_a \quad (3)$$

where A coefficient of 0.408 is used to convert MJ m^{-2} day^{-1} into mm day^{-1} and 0.0023 is the original coefficient of the Hargreaves equation [41]; ET_0 is in mm day^{-1}, T_{max}, T_{min} and T_{mean} are the maximum, minimum and mean monthly air temperatures (°C), respectively, and R_a is the extraterrestrial radiation (MJ m^{-2} day^{-1}) [41]. R_a depends on the Julian day number and latitude, and can be computed as described by Allen et al. (1998) [41].

The *SPEI* index proposed by Vicente-Serrano [42] is based on *SPI* but has the advantage of accounting for evapotranspiration due to temperature influence. Therefore, the *SPEI* is a difference between precipitation and potential evaporation [42].

The first step used to calculate the *SPEI* in this study was the estimation of *PET*. Then, the water balance equation was used to calculate the deficit (D_i). Furthermore, P_i and PET_i are the rainfall and evapotranspiration over time i, respectively, with the difference D_i the difference between precipitation P_i and PET_i as shown in Equation (4).

$$D_i = P_i - PET_i \quad (4)$$

Based on the D_i time series, the cumulative climate water balance series for different time scales was established, as shown in Equation (5).

$$D_n^k = \sum_{i=0}^{k-1}(P_{n-i} - PET_{n-i}), \qquad n \geq k \quad (5)$$

where k is the time scale, generally in months, and n is the number of calculations.

In the first version of *PET* calculation, the Thornthwaite (1948) method [43] was conducted in the case of data limitation. The Penman–Monteith method (Allen et al. 1998) is recommended because it considers more physical parameters such as, temperature, wind speed, and relative humidity [23,44]. Therefore, in this study, the FAO Penman–Monteith method was then used to calculate *PET*. If x is the cumulative series of D in a given time window, Vicente-Serrano et al. (2010) concluded that the log-logistic probability density

function has the best fit on the x-series values. The formulas of the density function and cumulative probability function of the three-parameter log-logistic probability distribution are expressed as Equations (6) and (7) [23,44].

$$f(x) = \frac{\beta}{\alpha}\left(\frac{x-\gamma}{\alpha}\right)^{\beta-1}\left[1+\left(\frac{x-\gamma}{\alpha}\right)^{\beta}\right]^{-2} \quad (6)$$

$$F(x) = \left[1+\left(\frac{\alpha}{x-\gamma}\right)\right]^{-1} \quad (7)$$

where the parameters α, β, and γ are equal to the parameters of the scale, shape, and location for the D_i values in the range of $\infty < D < \gamma$.

The cumulative probability density was transformed to a standard normal distribution to obtain the corresponding *SPEI* time series of change as shown in Equation (8).

$$SPEI = W - \frac{C_0 + C_1 W + C_0 W^2}{1 + d_1 W + d_2 W^2 + d_3 W^3} \quad (8)$$

where, $W = (-2\ln P)^{0.5}$, P is the probability of exceeding the determined moisture gain/loss, when $P \leq 0.5$, $P = 1 - F(x)$, when $P \geq 0.5$.

2.4. Correspondence Analysis (CA)

The CA is a multivariate technique primarily developed for the analysis of contingency table data [45]. Despite the fact that both principal component analysis (PCA) and CA display data in a low-dimensional plane, which explains the majority of the model's variance. Actually, it has been said that CA is a "weighted" or "generalized" PCA of a contingency table [46,47]. However, PCA identifies the variables that account for the most variance in the data set, whereas the goal of CA is to look at the relationships between the variables [48,49]. CA has been applied for detecting LULC change [50], for medical studies [51], and for water quality assessments [52]. Similar to variance, inertia is computed as the weighted sum of the squared distances of the rows to their barycenter.

3. Results

3.1. SPI 3-, SPI 6-, and SPI 9-Month Drought Pattern Analysis

The results of SPI 3- and SPI 6-month drought pattern analyses highlight the highest number of severe and moderate drought occurrences in Ca Mau during the period 1980–2019 (Figure 2a,b). Similarly, severe, moderate, and slight drought occurred most frequently for the SPI at 9 months (Figure 2c). It was also seen that most of the remaining meteorological stations often have a slight drought in cases of continuous drought for 3, 6, and 9 months.

At the short-term scale, results showed rapid change in the drought and wet conditions compared to the long term scales of 6-month or 9-month drought events. In all three cases, the terms for the SPI patterns show that Ca Mau province exhibits more months of drought occurrence (SPI ≤ -0.25), especially severe and moderate drought, than the rest of the provinces in the VMD. We expected that Ca Mau would have significantly different wet and dry characteristics than the rest of the VMD (at a significant 95%). Therefore, the symmetric plot of CA was conducted to (see Figure 2a–c), in which each row (row) and each column (column) are represented as one point on the map. In this study, the rows represent the drought and wet categories, while the columns represent the province names. The profile was calculated as the relative frequency of rows (rows profile) and columns (columns profile) in the contingency table. Therefore, rows or columns with similar profiles will be placed close together on the map.

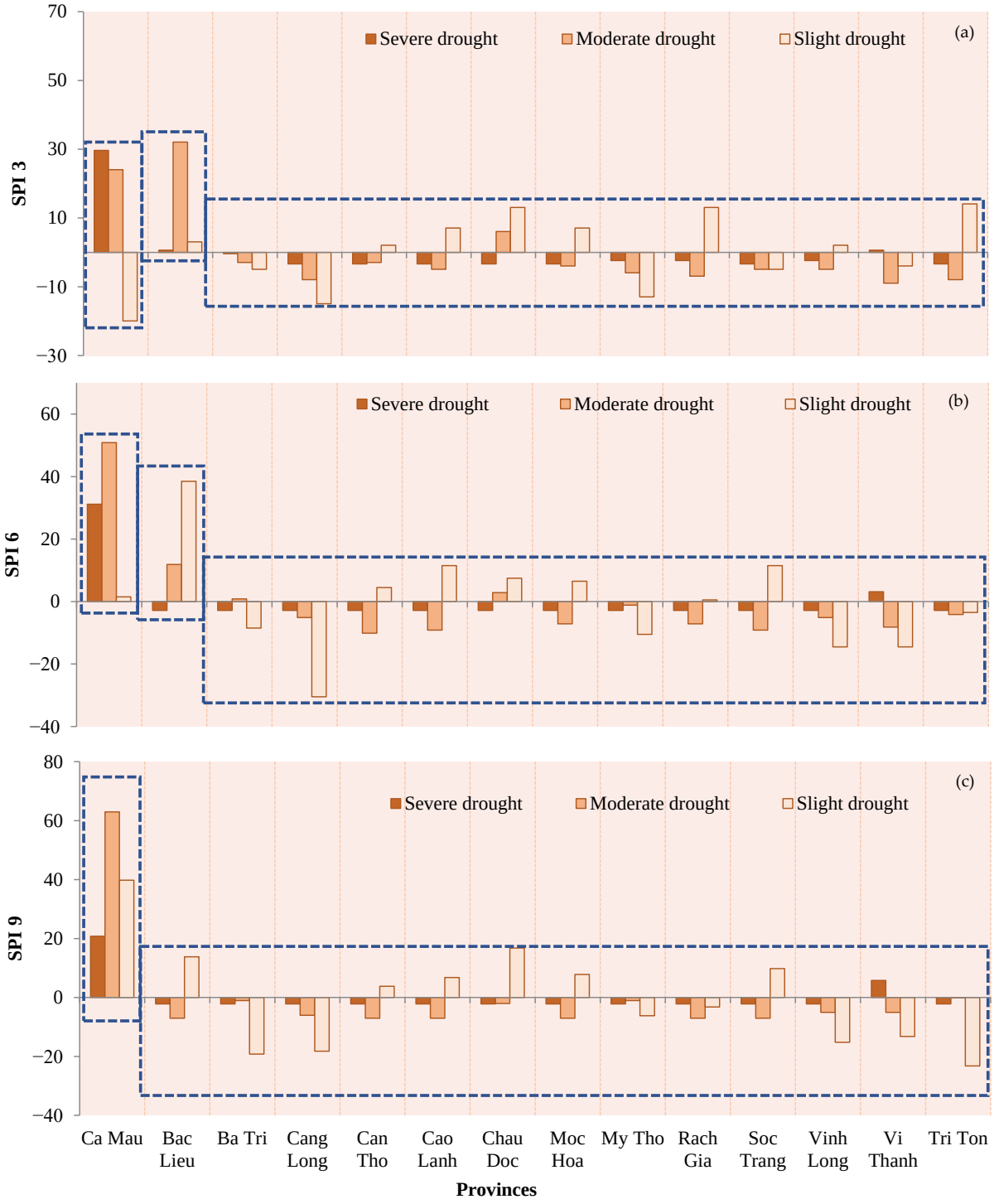

Figure 2. Number of occurrence events of various droughts at SPI 3 (**a**), SPI 6 (**b**), and SPI 9 (**c**) over 14 meteorological stations in the VMD.

Testing the dependency between rows (rows) and columns (columns) in the contingency table highlights that rows and columns have interdependencies with each other for the case of SPI 3, SPI 6, and SPI 9 consecutive month drought patterns. In this study, all three cases gave values of 90% or more. The graph of SPI 3- and SPI 6-drought patterns shows that the F1 axis is determined by the province of Ca Mau and severe drought. The SPI 9-month drought events symmetric plot shows that F1 is defined by the meteorological station in Ca Mau province with an extremely wet, severe, and moderate drought. Moreover, Ca Mau meteorological station is located geographically far away from the rest of

the stations in the VMD, which means that there are different dry and wet provinces. In addition, Figure 3a–c show that the Ca Mau meteorological station has characteristics of severe drought, mainly in the case of continuous drought at 3 months and 6 months. In the case of a 9-month drought pattern, the characteristics of severe drought, moderate drought, and extremely wet were discovered (SPI 9).

Despite the fact that calculated SPI 3 values oscillate more than SPI 6 and SP 9 levels between 1980 and 2019, all three assessment periods showed a similar tendency and can be divided into four periods: a dry weather prevailing from 1980 to 1990, followed by a wet weather period from 1991 to 2001, then alternately wet and dry weather period from 2002 to 2012, and finally a dry weather period from 2013 to 2019 (Figure 4).

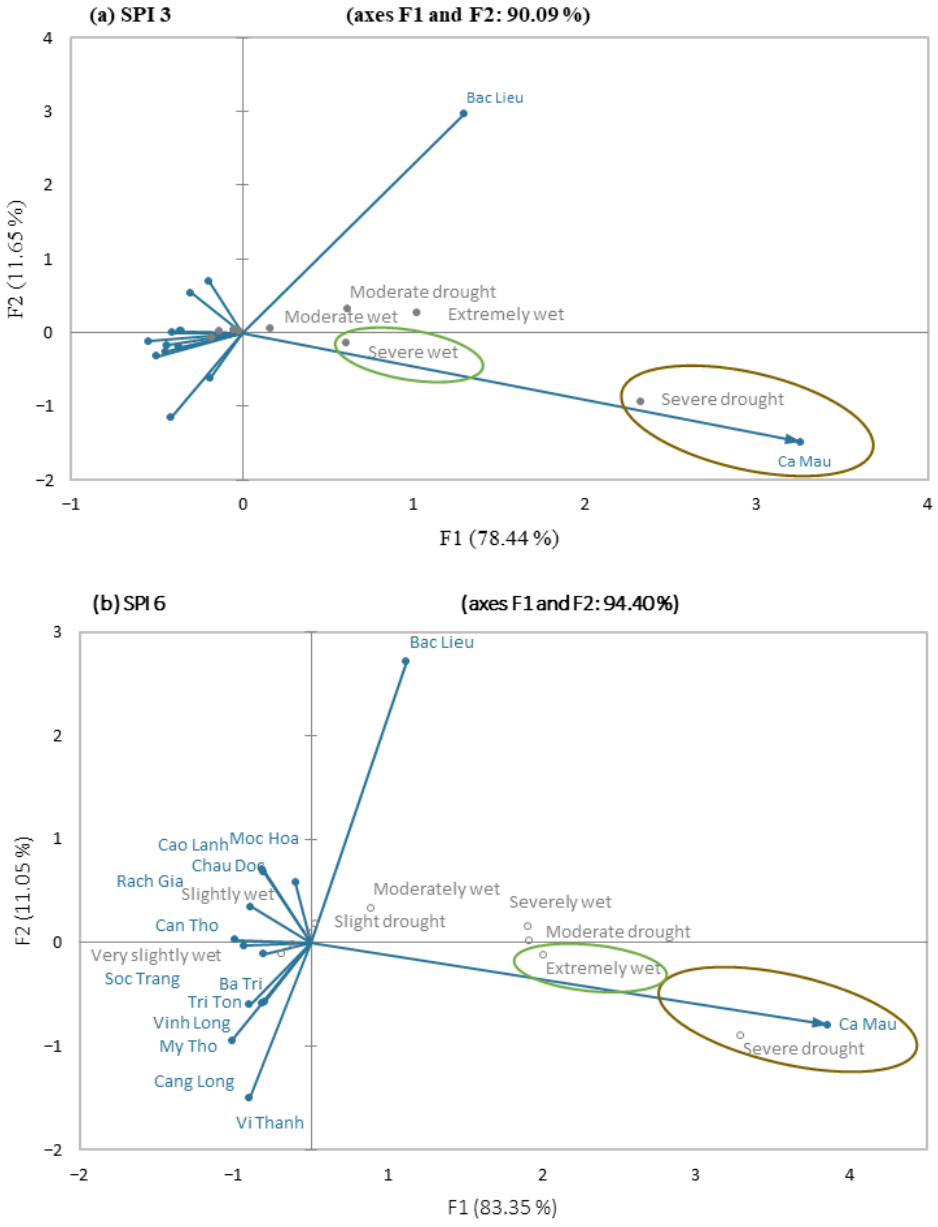

Figure 3. *Cont.*

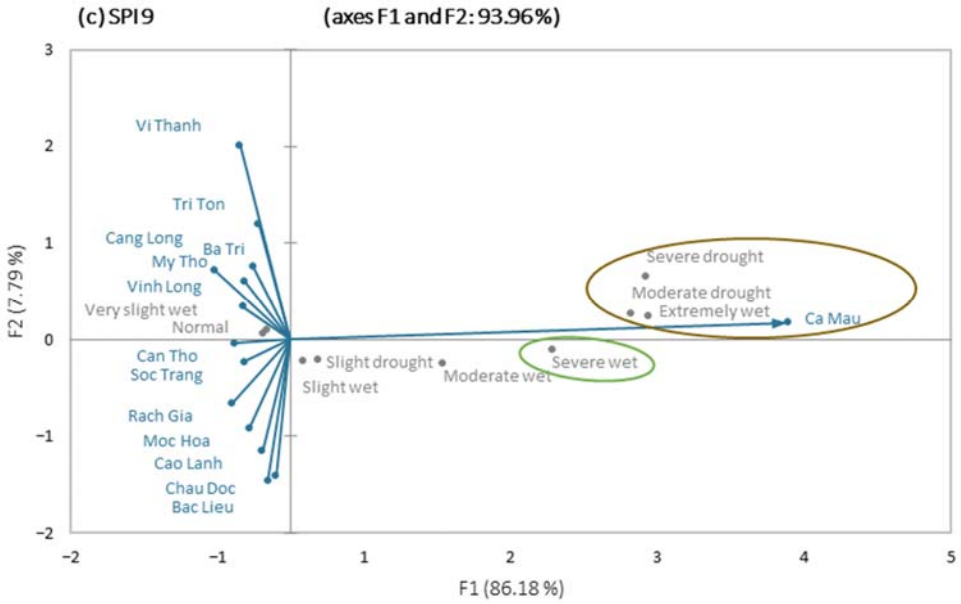

Figure 3. Symmetric plot of correspondence analysis for SPI 3 (**a**), SPI 6 (**b**), and SPI 9 (**c**).

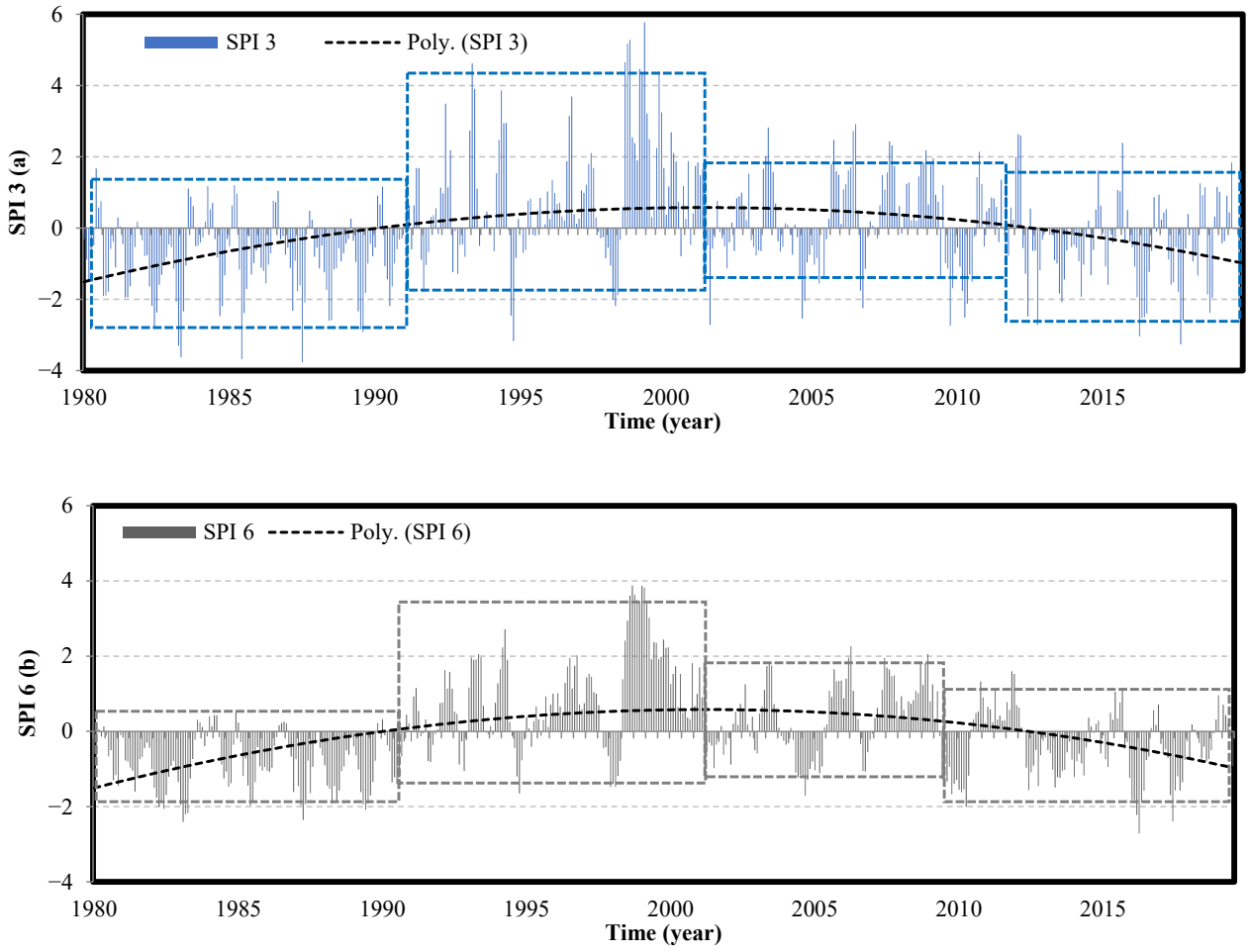

Figure 4. *Cont.*

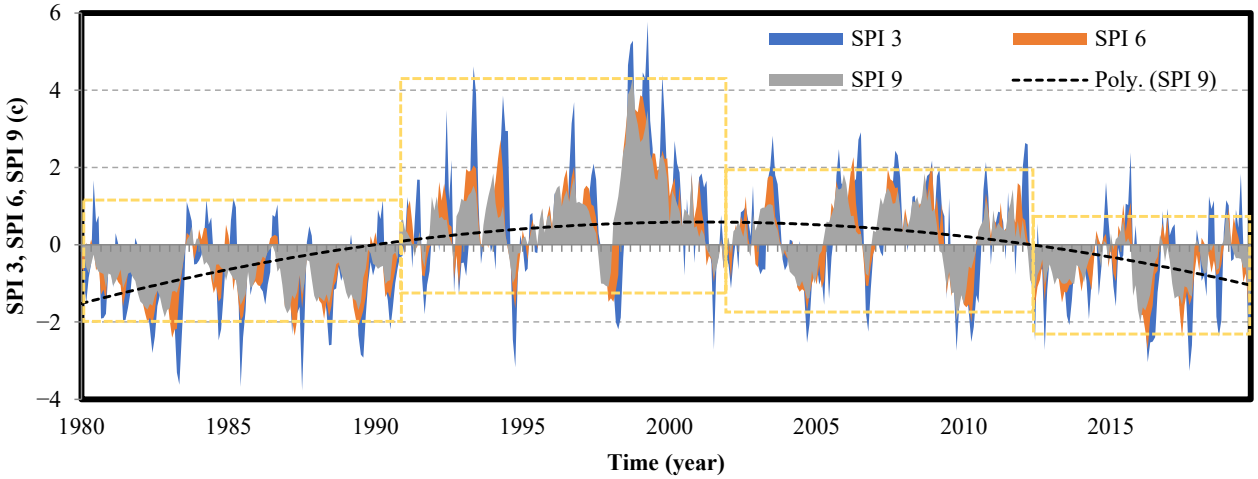

Figure 4. SPI 3 (**a**), SPI 6 (**b**), and SP 9 (**c**) values between 1980 and 2019.

During period 1: according to the SPI 3-month drought pattern, there was a drought lasting 8 months or longer every year; in particular, 11–12-month droughts occurred in the years 1982, 1988, and 1989. It was observed that droughts occurred even in the wet season in the period between 1980 and 1990. Continuous droughts of 6 months and 9 months were found in 1980, 1981, 1985, 1986, 1987, and 1988. Since 1989, there have been fewer months of drought, and period 2 has now begun.

During period 2: from the middle of 1998 until the beginning of 2001, there was a prolonged wet period. This time period also includes the longest La Nia effect. Before that, there was a period of strong El Niño influence from 1997 to mid-1998; however, wet months were found due to the influence of Tropical Storm Linda (1997) which was called Tropical Storm No. 5 in Vietnam. The event occurred in 1997 and destroyed 63,000 hectares of forest and 77,000 hectares of agricultural production, causing property damage in Ca Mau. According to research conducted by Ngu (2017) [53], between 1951 and 1997 Vietnam experienced an average of 5.3 tropical storms and tropical depressions per year during the El Niño years, which is two fewer than usual. Even though the number of storms that impact Vietnam is frequently lower than the national average and has been for many years, severe and extremely strong tropical storms can still occur [53].

During period 3: it was characterized by alternating periods of drought and wetness. There was a significant difference between the two seasons in special years with both severe drought and high humidity, such as in 1998, which showed both severe droughts in the dry season and high humidity in the wet season due to storm influence. There were months of extreme drought (SPI 3) from the end of 1997 to June 1998, whereas SPI 6 and SPI 9 showed less drought levels and duration than SPI 3, specifically SPI 6 and SPI 9. Furthermore, SPI 3 was quite sensitive and changed quickly when detecting periods of heavy drought or heavy wetness that appeared in a short period of time.

During period 4: despite the fact that this is a period of drought, the average magnitude of the drought decreased compared to the period between 1980 and 1990. Only a strong El Nino event created a severe to extreme drought from the end of 2015 to the end of 2016. On average, there were 7 months of drought each year and the distribution is irregular. During this period, the 2016 drought season was noticed. The drought and saline water intrusion in the dry season of 2015–2016 damaged 51,100 hectares of rice, 53,094 hectares of aquaculture, and caused drought in over 43,545 hectares of forests during these years. The severe drought in Ca Mau in 2015–2016 was caused by El Niño influence, causing significant damage to the production of winter—spring rice and rice on Ca Mau shrimp farming land [54]. Ca Mau has more than 49,000 hectares of rice damage, of which more than 35,000 ha are damaged on rice and shrimp tea, with the damaged area from 30–70% amounting to more than 6000 ha, and the damaged area from 70–100% amounting to more

than 27,000 ha; at the same time, over 12,000 ha of the winter–spring rice area was severely damaged due to a lack of water [55].

3.2. ARI and SPEI Analysis

The ARI and SPEI were estimated in the study for only the years 2000–2019 due to the study's limited use of temperature data (equivalent in time to period 4 in SPI analysis). Figures 5 and 6 display the findings of the ARI and SPEI analyses.

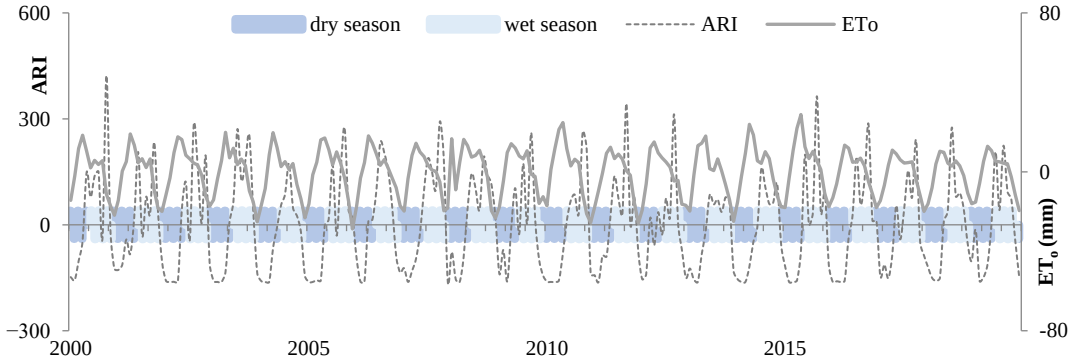

Figure 5. ARI variation both seasonally and yearly between 2000 and 2019.

When compared to SPI patterns, ARI shows very clear seasonal variation. As a result, the distribution of drought months follows the same pattern: typically, four months out of the year faced drought conditions (December to April next year). Therefore, we expected that SPEI could be used for drought assessment in the study area. Figure 6a–c displayed SPEI 3-, SPEI 6-, and SPEI 9-month drought patterns.

Dry and wet periods roughly coincide with SPI, according to SPEI findings from 2000 to 2019. The SPEI value, on the other hand, appears to be lower, indicating that the degree of extremes discovered is lower than that of the SPI. As a result, it is also essential to contemplate about the possibility of modifying the SPEI threshold.

3.3. Drought/Wet Occurrence Probabilities using SPI

The longest droughts, lasting 19 months, 29 months, and 41 months, were found in Ca Mau during the period 1980 and 2019 for SPI 3-month, SPI 6-month, and SPI 9-month, respectively. Drought conditions were at their worst in Ca Mau between 1980 and 1984, while wetness conditions were highest from 1998 to 2001. The longest wetness periods lasted 28 months, 34 months, and 35 months for SPI 3-month, SPI 6-month, and SPI 9-month, respectively (Table 2). It should be noted that wetness appears to last longer than drought in the short term, as measured by SPI 3. However, when considered over a longer period of time, such as SPI 9, the duration of drought occurrence was longer than the humidity in Ca Mau.

The drought and saline water intrusion in the dry season of 2019–2020 damaged nearly 21,000 hectares of rice and more than 51 hectares of crops; nearly 17,000 hectares of aquaculture; and nearly 21,000 households had difficulty accessing water for domestic use. There was a run of three consecutive drought months with the number of occurrences, especially in 2019–2022 [56].

If determined based on monthly probabilities, the probability of a drought event occurring (SPI 3-month ≤ -2) is 10%, and the probability of a wet event occurring (SPI 3-month ≥ 2) is 90%. Whereas, SPI 3-month values were determined to be ≤ -3.6 and ≥ 3.5, prospectively, for P = 1% and P = 99%, respectively (Figure 7). The probabilities of the SPI 6- and SPI 9-month drought patterns were also calculated (Figure A2).

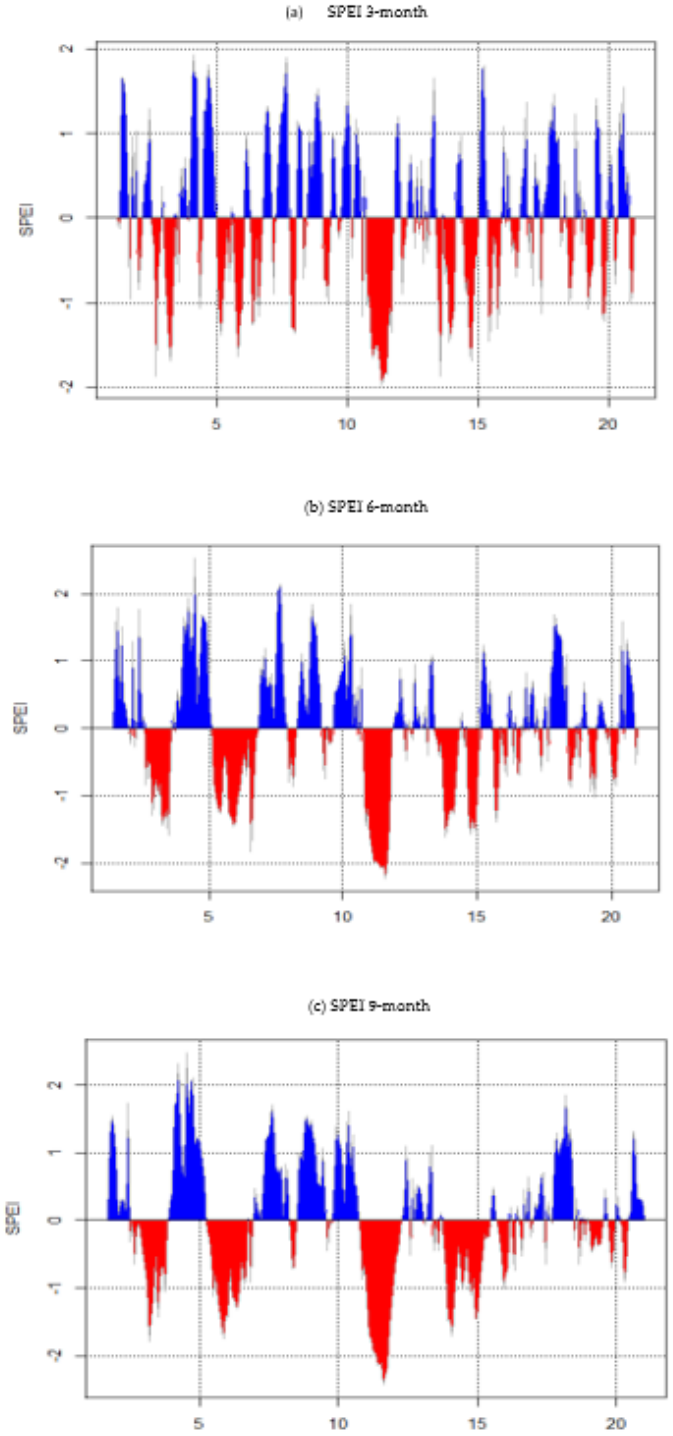

Figure 6. SPEI 3-month, SPEI 6-month, SPEI 9-month between 2000 and 2019.

The recent drought situation in Ca Mau has caused substantial damage to agriculture and other sectors. The local authorities are currently trying to formulate and implement a number of solutions. In the dry season of 2020, the whole VMD region suffered heavy damage due to drought. Yet, Ca Mau was the province which suffered the worst damage. The years of 2016 and 2019 are considered to be the most severe drought years in Ca Mau and the Mekong Delta.

Table 2. Number of drought and wet events using SPI duration in 1980–2019.

Characteristics	SPI 3-Month	SPI 6-Month	SPI 9-Month
Number of SPI ≤ -0.25	151	176	190
The first longest duration/occurrence times of drought (month)	19/Intensity (1)	29/1	41/1
Time occurrence first longest duration	1982–1983	1981–1983	1980–1984
Number of SPI ≥ 0.25	182	183	178
The first longest duration of wet condition	28/1	34/1	35/1
Time occurrence first long duration (month)	1998–2001	1998–2002	1998–2001

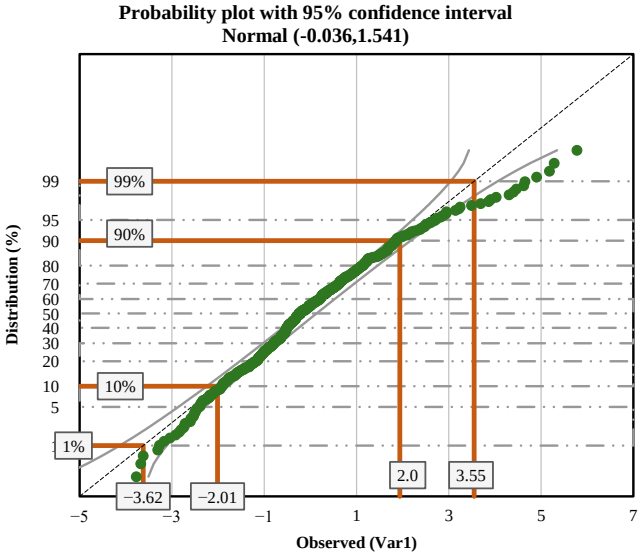

Figure 7. Probability plot with 95% confidence interval for SPI 3-month drought pattern.

4. Conclusions

Ca Mau exhibits a different drought and wetness distribution than the rest of the VMD. The characteristics of extreme drought and wetness extend beyond the duration of these events. It is possible to experience extreme drought during the dry season and high humidity during the wet season in the same year due to the effects of tropical storms. Although El Niño is responsible for the majority of drought events, local weather disturbances (storms or local wind) also have an impact on drought and wetness events in Ca Mau. ARI considers evapotranspiration levels in contrast to meteorological and hydrological drought as evaluated by SPI. Because temperature is factored into the computation of ARI and higher temperatures enhance evapotranspiration, the results for ARI deviate from the SPI projections. Both SPI and SPEI assessments contribute to an improved understanding of how unpredictable rainfall and meteorological anomaly conditions in Ca Mau are described by assessing severity levels and identifying the beginning and ending of droughts. The findings of our study are highly valuable in providing policy relevant information regarding extreme climate events and their possible impacts to crop yields. However, there are a number of limitations of this study as we did not consider climatic abnormalities such as El Niño and La Niña, and we also excluded using several other indexes such as the Keetch–Byram Drought Index (KBDI), which should be considered for future studies to obtain more precise information. Spatiotemporal maps showing dryness index distributions are also be vital to strengthen the scientific findings.

Author Contributions: Conceptualization, H.V.T.M., P.K., T.V.T., D.V.D., K.L. and R.A.; methodology, H.V.T.M., P.K., T.V.T., D.V.D., K.L. and T.G.H.; data curation, H.V.T.M. and T.G.H.; writing—original draft preparation, H.V.T.M., P.K., T.V.T., D.V.D., K.L., T.G.H. and R.A.; writing—review and editing, H.V.T.M., P.K., T.V.T., D.V.D., K.L. and R.A. All authors have read and agreed to the published version of the manuscript.

Funding: This research received no external funding.

Institutional Review Board Statement: Not applicable.

Informed Consent Statement: Not applicable.

Data Availability Statement: Not applicable.

Conflicts of Interest: The authors declare no conflict of interest.

Appendix A

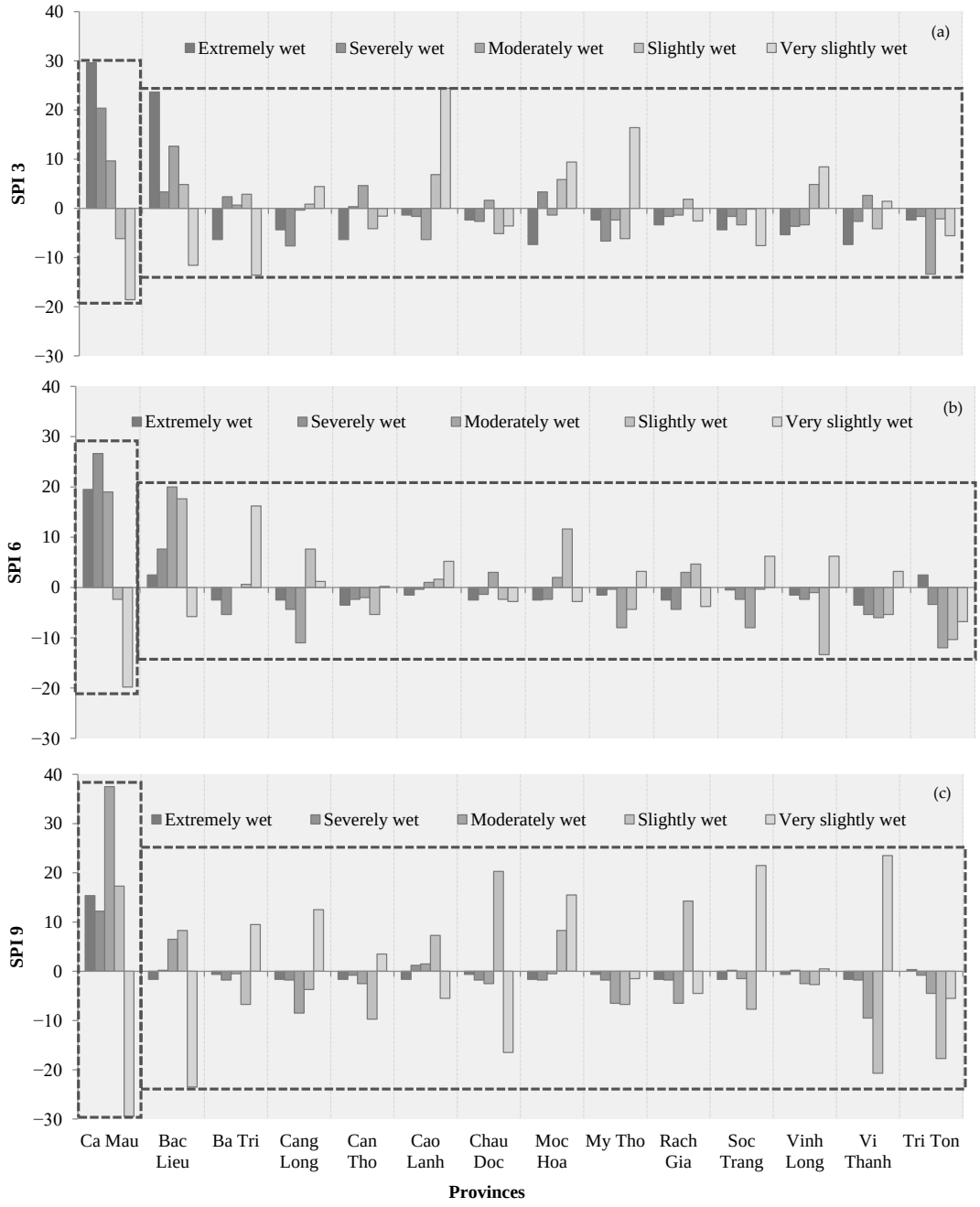

Figure A1. Number of occurrence events of various wet conditions at SPI 3 (**a**), SPI 6 (**b**), and SPI 9 (**c**) over 14 meteorological stations in the VMD.

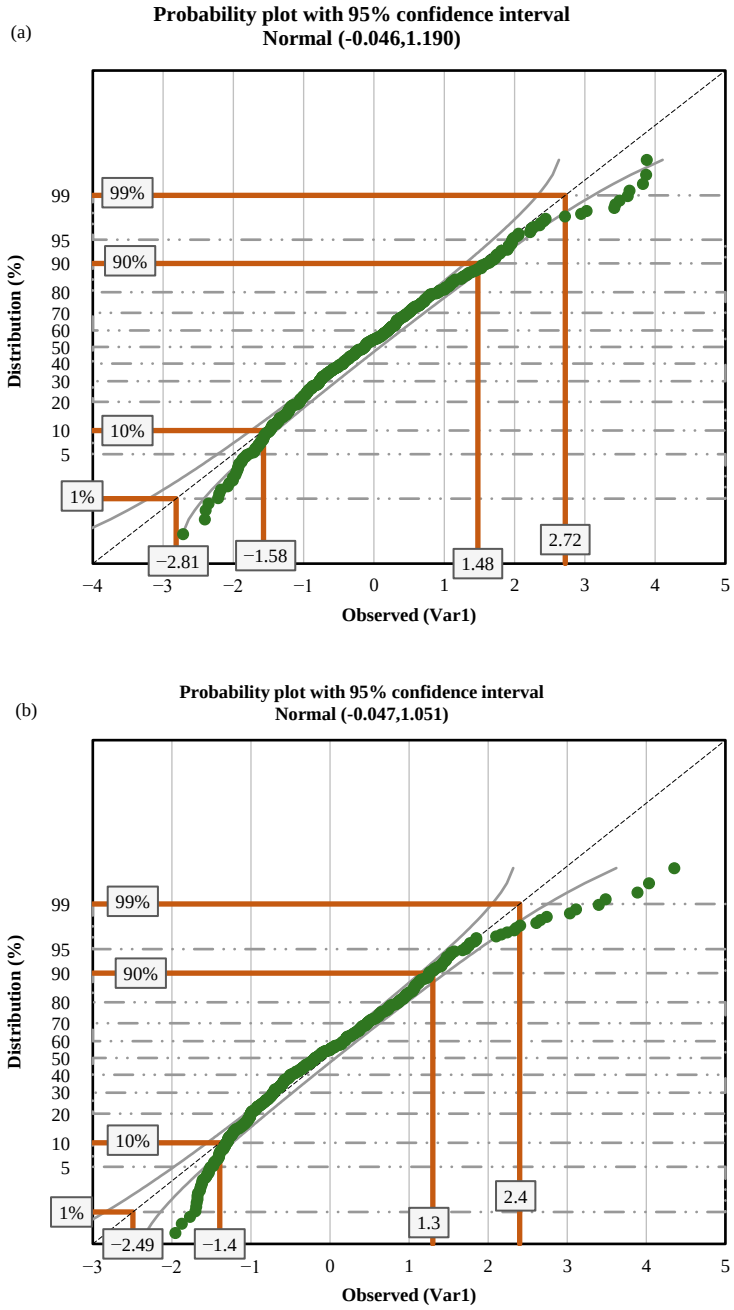

Figure A2. Probability plot with 95% confidence interval for (**a**) SPI 6 and (**b**) SPI 9.

References

1. Orimoloye, I.R.; Belle, J.A.; Olusola, A.O.; Busayo, E.T.; Ololade, O.O. Spatial Assessment of Drought Disasters, Vulnerability, Severity and Water Shortages: A Potential Drought Disaster Mitigation Strategy. *Nat. Hazards* **2021**, *105*, 2735–2754. [CrossRef]
2. Sivakumar, M.V. *Agricultural Drought—WMO Perspectives*; World Meteorological Organization: Geneva, Switzerland, 2011; p. 24.
3. Wilhite, D.A. Drought as a natural hazard: Concepts and definitions. In *Drought: A Global Assessment*; Wilhite, D.A., Ed.; Routledge: London, UK, 2000; Volume 1, pp. 3–18.
4. Palmer, W. Meteorological Drought. In *Drought: A Global Assessment*; Office of Climatology, U.S. Weather Bureau: Washington, DC, USA, 1965; pp. 45–58.
5. Pandžić, K.; Likso, T.; Curić, O.; Mesić, M.; Pejić, I.; Pasarić, Z. Drought Indices for the Zagreb-Grič Observatory with an Overview of Drought Damage in Agriculture in Croatia. *Theor. Appl. Climatol.* **2020**, *142*, 555–567. [CrossRef]
6. Hayes, M.J.; Alvord, C.; Lowrey, J. Drought indices. *Interm. West Clim. Summ.* **2007**, *3*, 2–6.
7. Heim, R.R., Jr. A Review of Twentieth-Century Drought Indices Used in the United States. *Bull. Am. Meteorol. Soc.* **2002**, *83*, 1149–1166. [CrossRef]

8. Ortega-Gaucin, D.; Ceballos-Tavares, J.A.; Ordoñez Sánchez, A.; Castellano-Bahena, H.V. Agricultural Drought Risk Assessment: A. Spatial Analysis of Hazard, Exposure, and Vulnerability in Zacatecas, Mexico. *Water* **2021**, *13*, 1431. [CrossRef]
9. Wilhite, D.A.; Glantz, M.H. Understanding: The Drought Phenomenon: The Role of Definitions. *Water Int.* **1985**, *10*, 111–120. [CrossRef]
10. Abbas, S.; Mayo, Z.A. Impact of Temperature and Rainfall on Rice Production in Punjab, Pakistan. *Environ. Dev. Sustain.* **2021**, *23*, 1706–1728. [CrossRef]
11. Ribeiro, A.F.; Russo, A.; Gouveia, C.M.; Páscoa, P. Modelling Drought-Related Yield Losses in Iberia Using Remote Sensing and Multiscalar Indices. *Theor. Appl. Climatol.* **2019**, *136*, 203–220. [CrossRef]
12. Madadgar, S.; AghaKouchak, A.; Farahmand, A.; Davis, S.J. Probabilistic Estimates of Drought Impacts on Agricultural Production. *Geophys. Res. Lett.* **2017**, *44*, 7799–7807. [CrossRef]
13. Wilhite, D.A. *Quantification of Agricultural Drought for Effective Drought Mitigation and Preparedness: Key Issues and Challenges*; World Meteorological Organization: Geneva, Switzerland, 2011.
14. Feng, P.; Wang, B.; Li Liu, D.; Yu, Q. Machine Learning-Based Integration of Remotely-Sensed Drought Factors Can Improve the Estimation of Agricultural Drought in South-Eastern Australia. *Agric. Syst.* **2019**, *173*, 303–316. [CrossRef]
15. Yahaya, T.I.; Muhammed, M. Assessing Rainfall Variability Impacts Using Agricultural Index (ARI) on Cassava Growth in Ilorin Area of Kwara State, Nigenia. *Int. J. Environ. Policy Issues. Geo-Stud. Forum* **2013**, *6*, 158–170.
16. Pandžić, K.; Likso, T.; Pejić, I.; Šarčević, H.; Pecina, M.; Šestak, I.; Tomšić, D.; Strelec Mahović, N. Application of the Self-Calibrated Palmer Drought Severity Index and Standardized Precipitation Index for Estimation of Drought Impact on Maize Grain Yield in Pannonian Part of Croatia. *Nat. Hazards* **2022**, *113*, 1237–1262. [CrossRef]
17. National Drought Mitigation Center (NDMC). Types of Drought. Available online: https://drought.unl.edu/Education/DroughtIn-depth/TypesofDrought.aspx (accessed on 9 July 2022).
18. Vicente-Serrano, S.M.; Beguería, S.; López-Moreno, J.I. A Multiscalar Drought Index Sensitive to Global Warming: The Standardized Precipitation Evapotranspiration Index. *J. Clim.* **2010**, *23*, 1696–1718. [CrossRef]
19. Wang, W.; Ertsen, M.W.; Svoboda, M.D.; Hafeez, M. Propagation of Drought: From Meteorological Drought to Agricultural and Hydrological Drought. *Adv. Meteorol.* **2016**, *2016*, 6547209. [CrossRef]
20. World Meteorological Organization (WMO). *International Meteorological Vocabulary*; WMO-No. 182; Secretariat of the World Meteorological Organization: Geneva, Switzerland, 1992; ISBN 978-92-63-02182-3.
21. Milanovic, M.; Gocic, M.L.; Trajkovic, S. Analysis of Meteorological and Agricultural Droughts in Serbia. *Facta Univ. Ser. Archit. Civ. Eng.* **2015**, *12*, 253–264. [CrossRef]
22. Beguería, S.; Vicente-Serrano, S.M.; Reig, F.; Latorre, B. Standardized Precipitation Evapotranspiration Index (SPEI) Revisited: Parameter Fitting, Evapotranspiration Models, Tools, Datasets and Drought Monitoring. *Int. J. Climatol.* **2014**, *34*, 3001–3023. [CrossRef]
23. Wang, W.; Zhu, Y.; Xu, R.; Liu, J. Drought Severity Change in China during 1961–2012 Indicated by SPI and SPEI. *Nat. Hazards* **2015**, *75*, 2437–2451. [CrossRef]
24. Ca Mau Web Portal. Ca Mau Overview. Available online: https://www.camau.gov.vn/wps/portal/gioi-thieu/tongquan/dieukientunhien (accessed on 17 September 2022).
25. Xuan, N.V.; Giang, N.N.L.; Ty, T.V.; Kumar, P.; Downes, N.K.; Nam, N.D.G.; Ngan, N.V.C.; Thinh, L.V.; Duy, D.V.; Avtar, R. Impacts of Dike Systems on Hydrological Regime in Vietnamese Mekong Delta. *Water Supply* **2022**. [CrossRef]
26. Van Ty, T.; Minh, H.V.T.; Avtar, R.; Kumar, P.; Van Hiep, H.; Kurasaki, M. Spatiotemporal Variations in Groundwater Levels and the Impact on Land Subsidence in CanTho, Vietnam. *Groundw. Sustain. Dev.* **2021**, *15*, 100680. [CrossRef]
27. Minh, H.V.T.; Lavane, K.; Ty, T.V.; Downes, N.K.; Hong, T.T.K.; Kumar, P. Evaluation of the Impact of Drought and Saline Water Intrusion on Rice Yields in the Mekong Delta, Vietnam. *Water* **2022**, *14*, 3499. [CrossRef]
28. McKee, T.B.; Doesken, N.J.; Kleist, J. *Drought Monitoring with Multiple Time Scales*; Applied Climatology, American Meteorological Society: Dallas, TX, USA, 1995; pp. 233–236.
29. McKee, T.B.; Doesken, N.J.; Kleist, J. The Relationship of Drought Frequency and Duration to Time Scales. In Proceedings of the 8th Conference on Applied Climatology, Anaheim, CA, USA, 17–22 January 1993; Volume 17, pp. 179–183.
30. Agnew, C. Using the SPI to Identify Drought. In Proceedings of the Drought Network News (1994-2001); National Drought Mitigation Center: UK, 2000; Volume 12, p. 8.
31. Soleimani, H.; Ahmadi, H.; Zehtabian, G. Comparison of Temporal and Spatial Trend of SPI, DI and CZI as Important Drought Indices to Map Using IDW Method in Taleghan Watershed. *Ann. Biol. Res.* **2013**, *4*, 46–55.
32. Ty, V.T.; Hoai, T.T.D.; Minh, V.T.H. Mapping Meteorological Drought in the Mekong Delta under Climate Change. *Can Univ. J. Sci.* **2015**, *2025*, 1980–2012.
33. Hồng, N.V.; Thơ, P.T.A.; Giai, N.S. Khả Năng Sử Dụng Chỉ Số SPI Trong Đánh Giá Ảnh Hưởng Của Điều Kiện Khô Hạn Đến Năng Suất Lúa ở Vùng Cần Thơ-Hậu Giang. *Tạp Chí Khoa Học Biến Đổi Khí Hậu* **2018**, *5*, 36–42.
34. Cheval, S. The Standardized Precipitation Index—An Overview. *Romanian J. Meteorol.* **2015**, *12*, 17–64.
35. Meleha, A.M.; Hassan, A.; El-Bialy, M.A.; El-Mansoury, M.A. Effect of Planting Dates and Planting Methods on Water Relations of Wheat. *Int. J. Agron.* **2020**, *2020*, 8864143. [CrossRef]
36. Ramana, G.V.; Suresh Kumar, R.; Balakrishna, P. *Restoration of Ecological Balance Through Regression Analysis in Kothapally Agricultural Fields*; Springer: Cham, Switerland, 2019; pp. 817–830.

37. Sayari, N.; Bannayan, M.; Alizadeh, A.; Farid, A. Using Drought Indices to Assess Climate Change Impacts on Drought Conditions in the Northeast of Iran (Case Study: Kashafrood Basin). *Meteorol. Appl.* **2013**, *20*, 115–127. [CrossRef]
38. Ghazalli, M.Z.; Nieuwolt, S. The Use of an Agricultural Rainfall Index in Malaysia. *Int. J. Biometeorol.* **1982**, *26*, 277–283. [CrossRef]
39. Paymard, P.; Yaghoubi, F.; Nouri, M.; Bannayan, M. Projecting Climate Change Impacts on Rainfed Wheat Yield, Water Demand, and Water Use Efficiency in Northeast Iran. *Theor. Appl. Climatol.* **2019**, *138*, 1361–1373. [CrossRef]
40. Nieuwolt, S. Estimating the Agricultural Risks of Tropical Rainfall. *Agric. For. Meteorol.* **1989**, *45*, 251–263. [CrossRef]
41. Allen, R.G.; Pereira, L.S.; Raes, D.; Smith, M. Crop Evapotranspiration-Guidelines for Computing Crop Water Requirements-FAO Irrigation and Drainage Paper 56. *Fao Rome* **1998**, *300*, D05109.
42. Saha, S.; Moorthi, S.; Pan, H.-L.; Wu, X.; Wang, J.; Nadiga, S.; Tripp, P.; Kistler, R.; Woollen, J.; Behringer, D. The NCEP Climate Forecast System Reanalysis. *Bull. Am. Meteorol. Soc.* **2010**, *91*, 1015–1058. [CrossRef]
43. Thornthwaite, C.W. An Approach toward a Rational Classification of Climate. *Geogr. Rev.* **1948**, *38*, 55–94. [CrossRef]
44. Abbasi, A.; Khalili, K.; Behmanesh, J.; Shirzad, A. Drought Monitoring and Prediction Using SPEI Index and Gene Expression Programming Model in the West of Urmia Lake. *Theor. Appl. Climatol.* **2019**, *138*, 553–567. [CrossRef]
45. Greenacre, M.J. *Theory and Applications of Correspondence Analysis*; Academic Press: London, UK, 1984.
46. Abdi, H.; Williams, L.J. Principal Component Analysis. *Wiley Interdiscip. Rev. Comput. Stat.* **2010**, *2*, 433–459. [CrossRef]
47. Greenacre, M.J. Correspondence Analysis. *Wiley Interdiscip. Rev. Comput. Stat.* **2010**, *2*, 613–619. [CrossRef]
48. Fellenberg, K.; Hauser, N.C.; Brors, B.; Neutzner, A.; Hoheisel, J.D.; Vingron, M. Correspondence Analysis Applied to Microarray Data. *Proc. Natl. Acad. Sci. USA* **2001**, *98*, 10781–10786. [CrossRef]
49. Pandžić, K. Principal Component Analysis of Precipitation in the Adriatic-Pannonian Area of Yugoslavia. *J. Climatol.* **1988**, *8*, 357–370. [CrossRef]
50. Cakir, H.I.; Khorram, S.; Nelson, S.A. Correspondence Analysis for Detecting Land Cover Change. *Remote Sens. Environ.* **2006**, *102*, 306–317. [CrossRef]
51. Greenacre, M. Correspondence Analysis in Medical Research. *Stat. Methods Med. Res.* **1992**, *1*, 97–117. [CrossRef]
52. Emad, A.M.S.; Eethar, M.A.-O. Assessment of Water Quality of Euphrates River Using Cluster Analysis. *J. Environ. Prot.* **2012**, *3*, 25650.
53. Ngu, N.D. El Niño 2015/2016 and Its Impact on Vietnam. *J. Clim. Chang. Sci.* **2017**, *1*, 29–35.
54. Seung Kyu, L.; Truong An, D. Evaluating Drought Events under Influence of El-Nino Phenomenon: A Case Study of Mekong Delta Area, Vietnam. *J. Agrometeorol.* **2018**, *20*, 275–279. [CrossRef]
55. Ca Mau Web Portal. Keeping the Forest in the Dry Season. Available online: https://www.camau.gov.vn/wps/portal (accessed on 20 September 2022).
56. Ca Mau Web Portal. Responding to Climate Change. Available online: https://daibieunhandan.vn/dia-phuong/ung-pho-voi-bien-doi-khi-hau-i263547/ (accessed on 19 September 2022).